THE JOURNAL OF PHYSICAL CHEMISTRY C

Article

pubs.acs.org/JPCC

Chalcogen Atom Interaction with Palladium and the Complex Molecule−Metal Interface in Thiol Self Assembly

Juanjuan Jia,[†,‡] Azzedine Bendounan,[§] Karine Chaouchi,[§] Stefan Kubsky,[§] Fausto Sirotti,[§] Luca Pasquali,[∥,⊥,#] and Vladimir A. Esaulov*[,†,‡]

[†]Institut des Sciences Moléculaires d'Orsay, Université-Paris Sud, 91405 Orsay, France

[‡]CNRS, UMR 8214, Institut des Sciences Moléculaires d'Orsay, ISMO, Bâtiment 351, Université Paris Sud, 91405 Orsay, France

[§]Synchrotron SOLEIL, L'Orme des Merisiers, Saint-Aubin, BP 48, F-91192 Gif-sur-Yvette Cedex, France

[∥]Dipartimento di Ingeneria 'E. Ferrari', Università di Modena e Reggio Emilia, Via Vignolese 905, 41125 Modena, Italy

[⊥]IOM-CNR, Science Park, 34149 Basovizza Trieste, Italy

[#]Department of Physics, University of Johannesburg, PO Box 524, Auckland Park 2006, South Africa

Supporting Information

ABSTRACT: In the case of reactive metals, on adsorption of organic chalcogenide molecules like thiols, chalcogenide-C bond scission can occur. Thus, the high reactivity of Pd leads to initial thiol dissociation and formation of a complex PdS interface layer on which thereafter thiol self-assembled monolayers (SAM) can form. In this context we investigate in detail the adsorption of S, Se, alkanethiols, and aromatic dithiols on Pd by photoemission with synchrotron radiation. The nature of the PdS and PdSe layers formed is studied, and thiol adsorption on Pd(111), PdS, and PdSe surfaces is investigated, along with interface characteristics. After initial strong sulfidation (selenization) in Na_2S(Se) solutions, a well-ordered surface PdS (PdSe) layer can be obtained by annealing. For S, annealing leads to formation of a PdS $(\sqrt{7} \times \sqrt{7})$R19.1° layer, whereas for Se, large domains of this structure are formed. Experiments suggest that in thiol adsorption the Pd−sulfide interface is not simply similar to the $(\sqrt{7} \times \sqrt{7})$R19.1° PdS layer but that modifications in this surface sulfide layer are induced. A similar effect is observed on the selenide interface layer. In addition, 1,4-benzenedimethanethiol adsorption on Pd is investigated with the aim of creation of thiol-terminated dithiol molecular layers. Unlike the case of surfaces like Au, no clear indication of a standing-up, thiol-terminated SAM was found. X-ray radiation damage effects are reported.

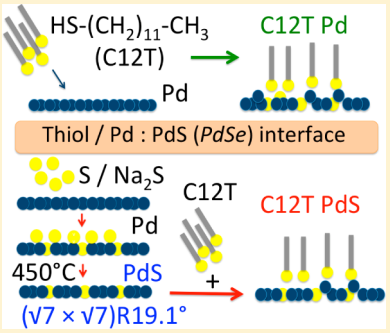

INTRODUCTION

In recent years there has been huge activity around organic−inorganic systems in various fields ranging from corrosion protection to molecular electronics. In all these cases the interface between an organic film and the substrate is one of the most important factors affecting the useful performance of the assembly. In this context, this work focuses on the case of palladium and its interaction with (1) chalcogenide atoms, (2) molecules bearing chalcogenide atoms, and finally (3) the complex chalcogenide interface layer formed in molecule adsorption when molecular dissociation processes in initial stages of adsorption occur. These systems are interesting and important for a number of reasons.

Palladium plays an important role in the chemical industry as a very efficient catalyst.[1−5] It is also used in hydrogen sensors because of its ability to absorb large amounts of hydrogen.[6] A major limitation in these applications is sulfur poisoning. Exposure to sulfur-containing compounds is well-known to deactivate Pd catalysts and Pd-based purification membranes[7−10] for hydrogen. Much effort is therefore devoted to circumvent this difficulty, and this requires a fundamental understanding of the interaction of sulfur with Pd surfaces.

Palladium has also been considered as an interesting substrate for self-assembled monolayers. Nuzzo's and Whiteside's groups[11,12] showed that alkanethiolate self-assembled monolayers (SAMs) formed on thin films of palladium form a better etch resistance layer for patterning SAMs than thin films on gold and other metals because of specific properties of alkanethiolates−Pd SAMs. Part of these specifics appear to be related to the fact that thiols do not simply form a self-assembled monolayer as on gold;[13−18] instead, there exists a PdS interface as a result of an initial reaction with the thiol accompanied by cleavage of the −S−C bond. Thereafter, ordered alkanethiol SAM formation occurs on this interface. Because of this, SAMs on palladium are more resistant to corrosion by solution-phase chemical etchants than those on gold. They were also found to be interesting in biotechnology, resisting invasion by cells for longer periods than SAMs on gold.

Received: July 15, 2014
Revised: October 2, 2014
Published: October 6, 2014

   dx.doi.org/10.1021/jp507051q | J. Phys. Chem. C 2014, 118, 24983−24994

Palladium nanoparticles[19] have been investigated in the context of catalytic applications,[20] hydrogen storage[21,22] and sensing applications.[23,24] Nanoparticles have to be stabilized with some capping agent, and in the context of thiol capping, in the case of Pd, the question of the nature of the interface arises. Alkanethiol-capped NPs have been described on the one hand as simply a metallic core covered by a thiol, or for instance by dioctyl disulfide layer,[25] and on the other hand as palladium sulfide NPs.[26] Recent work supports the view that, like bulk Pd, these are really a Pd core capped by a PdS layer on which the alkane SAM is adsorbed.[27,28] Interestingly, thiol capping of Pd NP's has been shown to improve in some cases their catalytic activity.

In a number of cases, attempts have been made to link nanoparticles, including Pd NPs using dithiols. Dithiol self-assembled monolayers are of interest in forming metal−organic molecule scaffolds.[29−31] The case of dithiol SAM formation on palladium surfaces has to our knowledge not been investigated. One of the issues in dithiol SAM assembly is the formation of intermediate lying down layers with both ends of the molecules chemisorbed on the substrate. It has been questioned if this could be an impediment to forming a standing-up SAM, although in recent work, on e.g., Au(111), we have shown that this should not be a problem.[32,33] In the case of palladium, this question acquires a new intriguing twist. In the initial phases, one thiol end might react with Pd, losing a sulfur atom, while the other end could by adsorbed. Thus, somewhat complex situations could arise, and it is not a priori clear if a thiol-ended SAM could be formed even if there is a "standing-up" molecular layer.

Despite a number of studies, the structure of the thiol/Pd(111) interface in the thiolate SAMs is still not clear. Characterization of sulfur layers on palladium is also not complete. In a more general context, interaction of Pd with heavier chalcogenides, Se and Te, has not been much investigated, as is also the case of SAMs with head groups involving these atoms rather than S.

In this work we therefore sought to clarify some of the unclear aspects of sulfidation of palladium as well as the related questions about formation of thiol and dithiol SAMs on its surface and the nature of the interface. To better delineate these problems, we now summarize some known facts on the basis of recent investigations.

S Adsorption and Self Assembly of Thiols on Pd. The formation of alkanethiol SAMs has been studied by several authors.[11,12,34] One of the first detailed studies of diverse chain-length alkanethiols[11,12] showed that fairly ordered SAMs could be obtained. This was inferred from infrared spectroscopy measurements. Their XPS investigation showed a difference from the "usual" structure on Au and some other surfaces: rather than observing a single S 2p related doublet,[35−39] a more complicated structure that could be attributed to two main doublet components[11,12,34] (with core level binding energies (CLBEs) at 162.3 and 163.2 eV for S $2p_{3/2}$) and a small extra feature was observed. It was concluded that the thiols were not adsorbed on the Pd(111) surface, but rather on a PdS interface layer and that the lower 162.1 eV doublet corresponded to the sulfide phase, whereas the higher binding energy component at 162.9 eV was assigned to the thiolate species.

In their analysis, the authors concluded that probably this interface layer may not be simply a single layer but: "It seems most likely that all the sulfur present at the interface cannot be confined to a two-dimensional surface structure, but rather, must reflect a metastable, compound palladium-sulfide interphase."[12] This point was more recently reinvestigated by Corthey et al.[34] and Carro et al.[41] and supported the above conclusions concerning the existence of an interface PdS layer. The assignments of the structures in the S 2p region, found at 162.1 eV and 162.9 eV, followed that of previous work.[11] These uncommented assignments appear on the one hand to be somewhat curious in that the thiolate CLBE is suggested to be 163.2 eV (or 162.9 eV) and not the lower 162.3 eV (or 162.1 eV) one, because in many cases of thiol adsorption on metals[13−16] and also on some semiconductors[39] it is closer to 162 eV. On the other hand, a rationalization of this could be that thiolate binding energies are usually higher than those for chemisorbed sulfur on, e.g., gold, which is closer to 161 eV.[40]

To discuss the possible nature of this PdS interface one needs to recall the characteristics of S adsorption on Pd. The interaction of sulfur on Pd has been the object of several investigations. Usually these investigations involved ultrahigh vacuum (UHV) adsorption onto Pd(111) by H_2S and in some cases S_2 dosing.[42−52] In one study, Pd was deposited on S layers. In some cases, sulfidation in solution using, e.g., Na_2S has been done. In the sub-monolayer range, two structures have been observed: the $(\sqrt{3} \times \sqrt{3})R30°$ phase and the more complex $(\sqrt{7} \times \sqrt{7})R19.1°$ phase. The $(\sqrt{3} \times \sqrt{3})R30°$ forms at lower coverage and lower temperatures and has a simple overlayer structure. The $(\sqrt{7} \times \sqrt{7})R19.1°$ phase has been observed upon annealing the $(\sqrt{3} \times \sqrt{3})R30°$ phase between 440 and 700 K and also in deposition of S_2 at 550 K.[45] The S coverage in this is considered to be 3/7. It is considered that this is a PdS atomic overlayer on the underlying Pd(111) surface. Several models of this structure have been proposed by Grillo et al.,[44] Liu et al.,[47] and Speller et al.[49,50] A detailed theoretical analysis by Alfonso[51,52] shows that the most stable is the Liu model, in which in the PdS overlayer the S atoms are a little below the Pd atoms and occupy off bridge sites.

To be able to better understand what one observes in XPS spectra it is essential to have a good knowledge of the S 2p CLBEs for different PdS surface structures and also of the Pd 3d core level. From the point of view of XPS investigations, S adsorption was studied by Rodriguez[42] in experiments on Pd evaporation onto sulfur layers and S_2 dosing on Pd(111). They observed a complex, multicomponent, S 2p peak, and this was decomposed into several components corresponding in particular to adsorption on bridge and hollow sites on the basis of an SCF calculation of S on a cluster. Here it would appear that one refers to low coverage and to the $(\sqrt{3} \times \sqrt{3})R30°$phase, whereas the CLBE for the $(\sqrt{7} \times \sqrt{7})R19.1°$ phase is not known. Corthey et al.[34] investigated S adsorption on a Pd film by sulfidation in Na_2S. The XPS spectrum in the S 2p region is also multicomponent, in which the S $2p_{3/2}$161.6 and 162.4 eV components deduced from fits were taken as suggesting the existence of PdS and PdS_2 contributions, respectively, while a third component at 163.3 eV was assigned to S_n species by analogy to the work of Rodriguez.[42]

A more recent theoretical work on thiol adsorption on Pd(111) by Carro et al.[41] discusses the formation of the thiol layer on a $(\sqrt{7} \times \sqrt{7})R19.1°$ phase, also mentioned earlier,[11] and concludes that most probably the thiols adsorb on this surface, *but with a reconstruction* wherein there are Pd adatoms extracted from the PdS layer and to which the thiols attach. There seems to be no experimental evidence yet to our knowledge supporting or refuting this conclusion.

Clearly the situation is rather complex, not easy to unravel, and still poses many questions. It is also interesting to point out that in some early investigations of methanethiol adsorption on other transition metals (Rh, W and Ni[53−55]) there are also observations of multicomponent S 2p spectra, which by analogy with the Pd case could be due to some type of interface sulfide layers. Similarly, some thiol[56] and dithiol[57] adsorption on Cu also involves initial dissociation and thereafter formation of the molecular layer on the surface with sulfur. Understanding the interfaces in these situations is thus very important.

In this work we reinvestigate this problem. We first performed a study of sulfur and selenium adsorption on Pd(111) and then studied dodecanethiol (C12T) adsorption on it. To attempt to delineate the characteristics of the would be PdS interface, we also studied C12T adsorption on both presulfidized and preselenized Pd surfaces. We used a selenized surface to try and delineate C12T adsorption on a different chalcogen passivated Pd surface, where, in photoemission, we can distinguish the molecule from the interface. We then investigate 1,4-benzenedimethanethiol (BDMT) interaction with Pd as an example of dithiol adsorption, previously investigated by us on Au(111).[35,58,59] Here we report the results of a high-resolution X-ray photoemission study complemented with low-energy electron diffraction (LEED) and ion-scattering investigations. These experiments will be described below.

EXPERIMENTAL METHOD

Experiments involved mostly high-resolution photoemission measurements at the Soleil synchrotron and some complementary studies by LEED and ion scattering.

Sample Preparation. Na_2S, Na_2Se, dodecanethiol, and BDMT were purchased from Sigma-Aldrich and used as supplied. Sulfidation and selenization of the clean Pd crystals (see below) were performed as in an earlier study[60] by immersion into a 0.1 mM Na_2S (Na_2Se) solution in a 0.1 molar aqueous NaOH. The clean Pd samples were extracted from the UHV preparation chamber under N_2 flow and immediately immersed into the solution. After immersion into the solution, the samples were dried by N_2 gas after rinsing with pure water. The samples were then transferred immediately into the analysis chamber.

Some experiments were also done for liquid-phase adsorption of dodecanethiol (C12T) for comparison with BDMT and earlier studies. In this case, the sample was immersed into a 1 mM ethanolic solution then rinsed and dried before analysis.

The adsorption of BDMT on Pd(111) was performed from liquid phase and vapor phase. In the case of vapor phase, the Pd single crystal undergoes sputtering and annealing cycles, and the cleanliness is checked by time of flight direct recoil spectroscopy (TOF-DRS). The BDMT molecules were introduced into the chamber from a sealed pyrex tube by opening a valve and by controlling the vacuum pressure through a gauge to define the dose. Characteristics of BDMT adsorption were then studied by TOF-DRS. Alternatively, the prepared sample was put into a sealed box filled with N_2 and then taken to the Tempo beamline at the Soleil synchrotron. In the case of liquid-phase adsorption, the sample was immersed into 1 mM BDMT solution in degassed *n*-hexane and then rinsed in *n*-hexane. It was observed earlier for BDMT adsorption on Au(111) that the best self-assembly results were obtained when the BDMT solution in *n*-hexane was heated to 60 °C. In this series of measurements we used both heated and non-heated solutions.

Time of Flight Direct Recoil Spectroscopy. The TOF-DRS[61] investigation of Pd sulfidation was performed in our own laboratory in Orsay. This technique is very sensitive to top surface atoms, produces negligible damage to the organic layer, and has been useful for detecting S atoms on S-terminated dithiol SAMs.[57,62]

The Pd crystal was prepared by several cycles of Ar^+ sputtering and annealing at 600 °C. It was then exposed to BDMT vapors and analyzed by ion scattering. A pulsed 4 keV Ar^+ beam was incident on the surface at typically 7° and 20° incidence with respect to the surface plane. Measurements were performed for a 45° scattering angle from the incident beam direction. Time of flight spectra of scattered and fast forward recoiled atoms were recorded, using a multichannel plate detector set at the end of a 1.70 m flight tube.

Between measurements, after high BDMT exposure, the chamber was baked out to eliminate BDMT from the walls.

Photoemission. The photoemission experiments were performed in the UHV end-station of the TEMPO beamline at Synchrotron SOLEIL using a Scienta SE2002 spectrometer. The Pd crystal was prepared in the preparation chamber by cycles of Ar^+ sputtering and annealing at 600 °C and finally flashing to high temperature in an O_2 atmosphere, which removes C residues. The energy resolution in these measurements was better than 50 meV. In the following, the binding energies in the XPS spectra were calibrated with respect to the Au($4f_{7/2}$) peak, set at 84 eV, using a Au(111) monocrystal. The calibration error is estimated to be of 50 meV. With few exceptions, we used photon energies so that the final kinetic energy would be around 100 eV to minimize attenuation due to scattering of electrons in the organic layers. The photon energies were 466 eV for Pd 3d core level, 466 and 260 eV for S 2p, and 380 eV for C 1s.

SULFUR AND SELENIUM ADSORPTION ON PD(111)

In the following sections we shall first describe data on sulfur and selenium interaction with Pd, followed in the next sections by results for C12T and BDMT adsorption. Some other results are given in the Supporting Information, and the figures from the Supporting Information are referenced as Figure S*n*.

Sulfur Adsorption. An overview XPS spectrum for the clean Pd(111) surface is shown in Figure 1. The clean Pd spectrum (blue line) shows an intense peak at about 334.8 eV which is due to the Pd $3d_{5/2}$ core level and the broader small structure at about 55 eV due to Pd 4p. Other structures are labeled in the figure. A detailed view of the Pd 4p region taken at a photon energy of 466 eV is shown in Figure 1 inset, and that of Pd 3d is shown in Figure 2a.

After incubation in the Na_2S solution (Figure 1), we see a clear structure with a binding energy of around 162 eV, related to the S atom. We saw in some cases a C 1s peak probably resulting from passage through air before introduction into the chamber from the solution. In some cases after immersion, we saw in the XPS spectrum a Na 2p structure at about 30 eV and a Na 2s core level structure at about 64 eV. This effect appears to be related to rinsing. However, after the sample was heated to about 350 °C, the C and Na peak disappear but S remains (Figure 1). Further heating of the samples up to 450 °C did not show any other changes in the surface composition. The

dx.doi.org/10.1021/jp507051q | J. Phys. Chem. C 2014, 118, 24983−24994

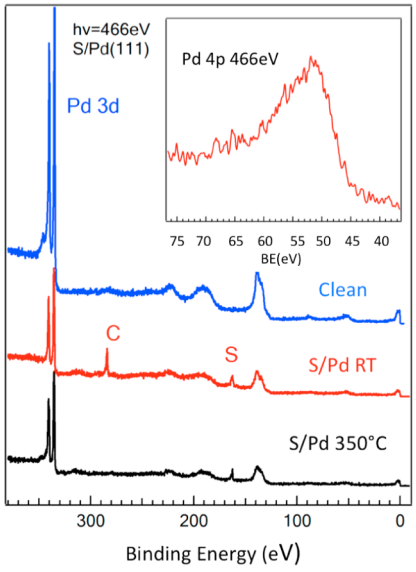

Figure 1. XPS overview spectrum of Pd(111): clean surface (blue line), with initial S adsorption on the surface (red line), and after heating to 350 °C (black line). Inset: XPS spectra of the Pd 4p region.

intensity of the S 2p peak as compared to that of the Pd 3d peak (taken from peak areas) decreases after heating.

The Pd 3d main region evolution under different situations is shown in Figure 2. The Pd 3d peak for clean Pd(111) was fitted with two components with an asymmetric profile, shown in Figure 2a. These two components are Pd_S (surface) and Pd_B (bulk) at 334.6 and 334.9 eV respectively. We estimate an error on the peak positions in the fits described in this paper to be less than 50 meV. The energy difference between bulk and surface components given in earlier experiments and calculations is 0.28 and 0.30 eV.[63,64] Note that from this spectrum itself it would be difficult to make a reasonable separation into these components. This fit was actually performed on the basis of a comparison with the sulfidized surface, in which case one can distinguish the bulk component. On sulfidation, the surface component is removed, as in the case of Au.[33,35,58−60]

After S adsorption, the Pd 3d peak shifts toward higher energy, as shown in Figure 2b,c. The shift is quite large, and one can notice that the Pd bulk component is drastically attenuated. This sulfidized Pd $3d_{5/2}$ peak is slightly asymmetric, with a low-energy shoulder, and could be fitted by two main components (Figure 2b) at 335.20 and 335.65 eV, and with a third very small one corresponding to the bulk component. This suggests the existence of differently coordinated atoms in the sulfide layer. Note that in all these fits we maintained the same line shape.

After the sample is heated to 350 °C, the Pd 3d peak shifts back to lower energy and an obvious shoulder at lower energy can be seen (Figure 2c). It is this shoulder that was used as a guideline to separate the clean Pd 3d peak into bulk and surface components. The Pd peak after sulfidation and heating was fitted with two asymmetric profiles corresponding to the bulk component at 334.90 eV and the sulfide component at 335.48 eV.

Figure 3 shows XPS spectra of S 2p core level structure taken at 466 eV photon energy for grazing and normal incidence,

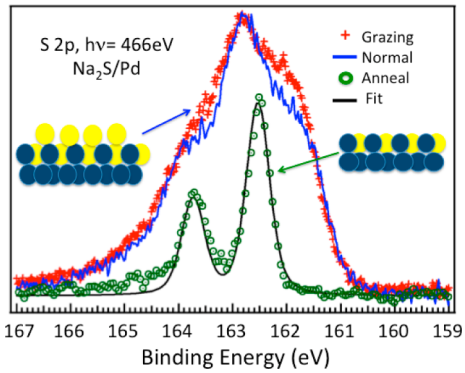

Figure 3. XPS spectrum in the S 2p region before (blue, normal emission; red, grazing emission) and after annealing to 450 °C (green line).

after a Shirley background subtraction. We see a multicomponent broad spectrum, similar in shape to that of earlier reports.[11,12,34] One can see that the lower-energy shoulder is more pronounced for grazing incidence. While not large, the difference is clearly noticeable, suggesting that the lower-energy shoulder corresponds to a more surface component, whereas the central component is from an underlying phase. These observations correlate well with the above indication from the Pd 3d core level shape, i.e., that there is more than one component in the sulfide layer. We will return to this point later. Note that we did not observe any strong oxidation, which is known to result in a structure at about 168 eV, which was not observed in our spectra.

A fit of the S 2p XPS spectra was performed and is shown in Supporting Information Figure S1 after a Shirley background

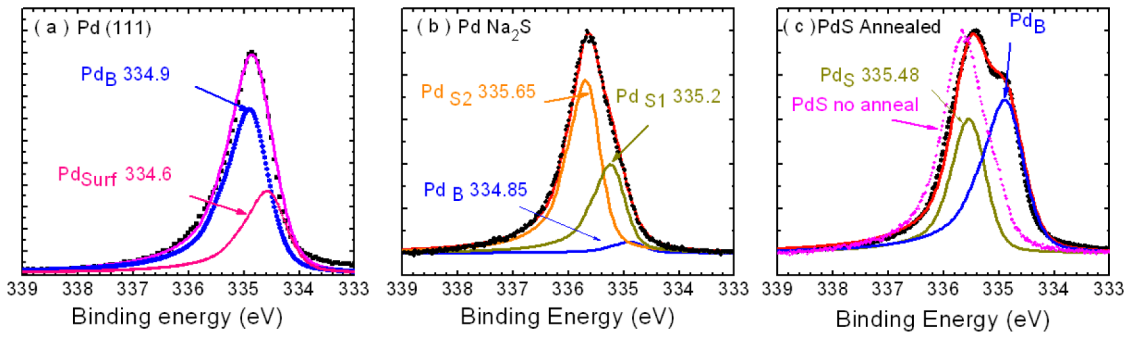

Figure 2. XPS spectra of Pd $3d_{5/2}$: (a) clean surface, (b) after initial S adsorption, and (c) after S adsorption and heating to 350 °C. In (c), the dashed line is the spectrum after initial adsorption.

dx.doi.org/10.1021/jp507051q | J. Phys. Chem. C 2014, 118, 24983−24994

subtraction using Voigt profiles. As usual, we set a 1.2 eV spin orbit splitting and a 1:2 intensity ratio of the two S $2p_{1/2}$ and $2p_{3/2}$ components. In the following, for S 2p and later for Se 3d we will refer to the doublets by the energy of the S $2p_{3/2}$ (Se $3d_{5/2}$) component. The peak was fitted by using two main doublets at 161.70 and 162.68 eV and introducing some smaller components (see Figure S1). The existence of the main components is in agreement with earlier works,[11,34] as mentioned in the introduction.

When the sulfidized sample is heated, the S 2p region spectrum changes strongly, showing essentially only one doublet after heating (green line) at 162.47 eV. A fit of this doublet is shown in Figure 3. No changes in these XPS spectra related to damage were observed prior to and after heating.

From earlier reports[44,47,50] it is known that upon annealing of sulfur adlayers on Pd there appears a $(\sqrt{7} \times \sqrt{7})$R19.1° PdS structure (in the following we refer to it simply as the $\sqrt{7}$ structure). To verify the nature of our layer after annealing, we performed a LEED study. Prior to annealing to 350 °C we did not observe any clear LEED patterns. After annealing, we see a clear LEED pattern (Figure 4) that is similar to the one

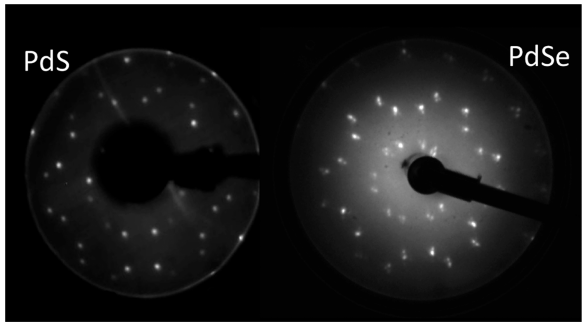

Figure 4. LEED patterns of the $(\sqrt{7} \times \sqrt{7})$R19.1° structure for PdS after annealing to 450 °C and PdSe after annealing to 600 °C.

reported earlier for the $\sqrt{7}$ structure. We did not observe the $(\sqrt{3} \times \sqrt{3})$R30° structure of S adsorption on Pd surface before annealing or after annealing to higher temperatures. The $(\sqrt{3} \times \sqrt{3})$R30° structure appears to correspond to initial submonolayer adsorption, and we would not expect it in strong sulfidation. In some cases a small feature at the right appeared in the spectra, at about 161.5 eV, probably due to insufficient heating and could correspond to some S atoms in another configuration on this layer.

We thus observed the formation of the $\sqrt{7}$ PdS surface sulfide layer and its characteristic XPS spectrum consists of a doublet at 162.45 eV. The structure proposed by Liu et al.[47] and which from calculations of Alfonso[52] appears to be the most stable indicates that this corresponds to a PdS atomic layer with S atoms at slightly off bridge sites.

From these observations one could conclude that upon initial strong sulfidation in the Na_2S solution, a sulfide underlayer is formed with S 2p CLBEs about 0.21 eV higher than for the $\sqrt{7}$ structure and a S overlayer with lower CLBEs. This could include S adsorbed on top of the surface sulfide and eventually a polymeric S_n component. Concerning the polymeric component, note that in earlier work[34] this was assigned to a higher-energy component (lying at 163.3 eV). However, in the case of Au the same authors assigned polymeric S_n components to a structure at a binding energy of 162.1 eV.[47]

Selenium Adsorption. A similar investigation was performed for Se adsorption on Pd(111). Figure 5 shows the evolution of the Pd 3d peak upon selenization and after annealing. As for sulfur, one sees a strong core level shift of Pd 3d. This decreases upon heating. Fits of the spectra, decomposing these into bulk and selenide components, using the same procedure as for sulfur are shown in Figure 6. After initial selenization the spectrum could be fit with just one component.

In the case of Se 3d we also observed, as for S, a multicomponent spectrum, which here is located on a broad structure corresponding to Pd 4p as shown in Supporting Information Figure S2. Figure 6a,b shows XPS spectra of Se 3d core level structure taken at 466 eV photon energy for grazing and normal incidence, after subtraction of a Shirley background and the Pd 4p contribution, using the spectrum in Figure 1 as the guideline. One can see that the lower-energy shoulder is more pronounced for grazing incidence, showing that it corresponds to a more surface component, whereas the central component is from an underlying phase. This is similar to the sulfur case described earlier.

Fits of the Se 3d XPS spectra are shown. We set a 0.86 eV spin orbit splitting and a branching ratio of 0.66 of the two $3d_{5/2}$ and $3d_{3/2}$ components. The fit includes two main broad doublets at 54.27 and 55 eV and some small components at 56 and 57.2 eV.

After the sample is heated to 300 °C, we see a narrowing of the spectrum and appearance of finer structures, but the spectrum is still composed of several doublet components, as shown by the fits in Figure 6c. Heating to 500 °C leads to a change in intensity of the different components (Figure 6d,e), with an attenuation of the 54.65 eV peak and dominance of the 53.90 eV peak. Here also we see that the lower binding energy peak is more pronounced for grazing incidence, suggesting that it corresponds to a more surface component, whereas the

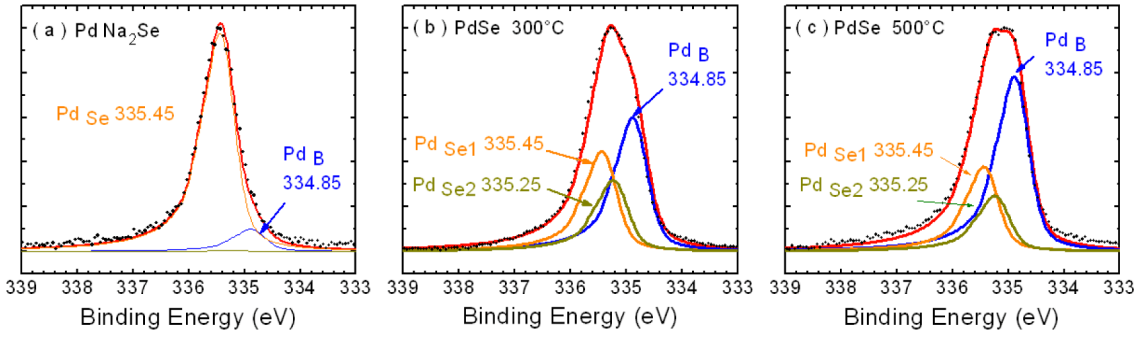

Figure 5. XPS spectra of the Pd 3d region after (a) initial immersion into the Na_2Se solution, (b) heating to 300 °C, and (c) heating to 500 °C.

dx.doi.org/10.1021/jp507051q | J. Phys. Chem. C 2014, 118, 24983−24994

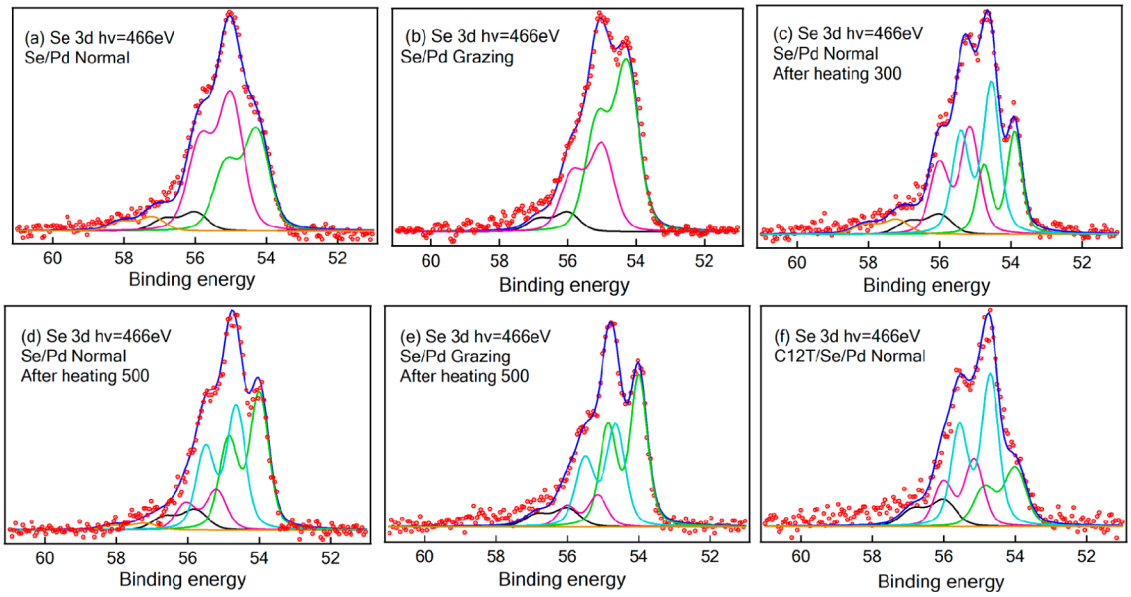

Figure 6. XPS in the Se 3d region after (a,b) initial selenization and for normal (a) and grazing (b) emission; (c) after heating to 300 °C and (d,e) heating to 500 °C shown for normal (d) and grazing (e) emission. (f) Spectrum after C12T adsorption on the selenized surface (see text).

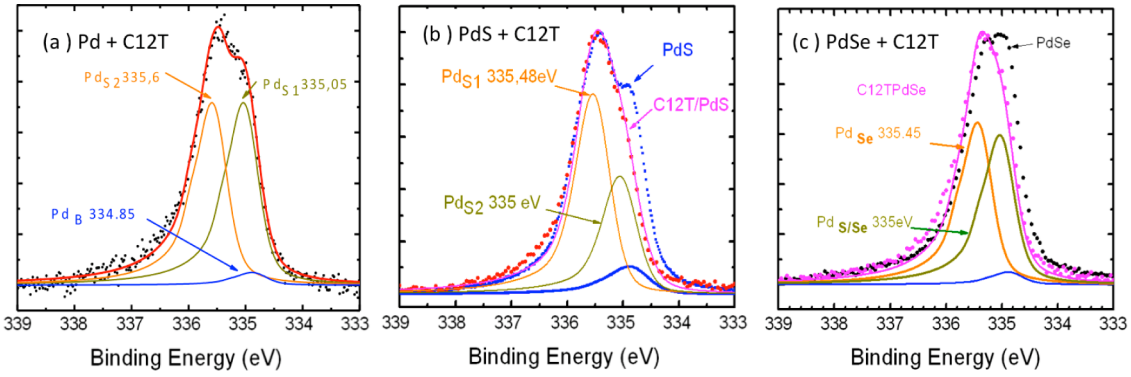

Figure 7. XPS spectra in the (a) Pd 3d region in the case of C12 molecules adsorption and (b) Pd 3d region in the case of C12 molecules adsorption on PdS (see text) compared to the one for the initial PdS surface. (c) Pd 3d region in the case of C12 molecules adsorption on PdSe (see text) compared to the one for the initial PdSe surface. Other lines are components of fits as discussed in the text.

central peak at 54.65 eV is from an underlying phase. As for sulfur no changes in these XPS spectra related to damage were observed prior to and after heating.

Some LEED images were taken after heating the selenized sample, and these images are shown in Figure 4b. After the sample is heated to 300 °C, a clear LEED pattern is observed, but there is still a diffuse background. It becomes sharper after heating to 500 °C. Heating to 700 °C did not produce further changes. The LEED pattern is similar to the one for sulfidized Pd corresponding to the $\sqrt{7}$ structure but has a more complex structure, with widely spaced rotated domains. One could try to relate this feature to the existence of the two Se CLBE peaks possibly corresponding to atoms in the $\sqrt{7}$ structure and also interdomain atoms with a different arrangement. This is similar to what has been reported for S adsorption on Cu(100).[65,66] However, given the similar intensities of the two peaks in Figure 6, it is not obvious that such boundary atoms could be responsible for this result. It is also not a priori obvious that Se atoms are all equivalently placed in the basic $\sqrt{7}$ structure as for sulfur or if, e.g., some vertical displacements could occur. We will not discuss this question in more detail here.

Finally, some preliminary measurements were made in the valence band (VB) region for the different conditions described above and are given in the Supporting Information Figure S3.

DODECANETHIOL ADSORPTION ON PD(111), PDS, AND PDSE SURFACES

In this section we discuss a series of experiments on C12T adsorption on Pd(111) and also some experiments that were performed after prior sulfidation and selenization of the Pd surface. This was done in an attempt to delineate interface-related characteristics because it has been suggested that the alkanethiol SAM is formed on a palladium sulfide interface layer.

C12T on Pd(111). After C12T adsorption, the Pd 3d peak changes shape and shifts to higher binding energies, as in the case of sulfur adsorption as shown in Figure 7a. The C 1s peak is found to be at 284.68 eV and is shown in Supporting Information Figure S4. The Pd 3d spectrum was fitted as for sulfur with mainly two sulfide components at 335.05 and 335.6 eV. Thus, this shows existence of differently coordinated Pd atoms in the sulfide.

dx.doi.org/10.1021/jp507051q | J. Phys. Chem. C 2014, 118, 24983−24994

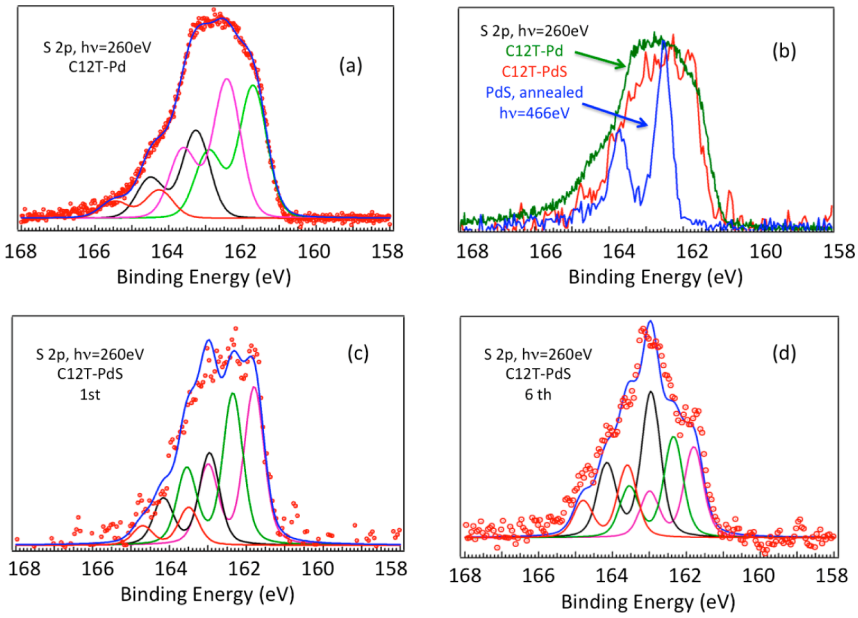

Figure 8. (a) XPS S 2p spectrum for C12T adsorption on a pristine Pd(111) surface. (b) Comparison of S 2p spectra for the $\sqrt{7}$ PdS surface after annealing (blue line), PdS with adsorbed C12T molecules (red line), and clean Pd(111) with C12T molecules (green line). Lines correspond to fits described in the text. Fit of the (c) first scan of the C12T-PdS spectrum and (d) last scan illustrating X-ray radiation damage effects.

In the case of the S 2p peak, we observe a broad, clearly multicomponent structure (Figure 8a). The general features are similar to the results reported earlier.[11,34] One can subdivide this spectrum into two major, rather broad doublets at 161.71 and 162.45 eV and smaller doublets at 163.26 and 164.26 eV. The large width presumably implies that we are really fitting several close-lying components. We will discuss the assignment of the thiolate and sulfide components in the next section.

As is known from the literature, irradiation of alkanethiol components leads to the appearance of free alkanethiols trapped within the SAM that may also be −S−S bonded, and this leads to the appearance of a radiation damage-induced structure at a binding energy of about 163.5 eV. We checked as a function of sucessive scanning over the energy range of the spectrum that no significant changes occurred in the spectrum shape and intensity (Supporting Information Figure S5).

C12T on PdS. Because it has been suggested[11,41] that thiol SAM formation is accompanied by formation of a PdS layer and that this layer could have characteristics of the $\sqrt{7}$ structure, we performed an experiment in which we preadsorbed S on Pd and annealed the sulfide layer to obtain the $\sqrt{7}$ PdS surface, as described above. This was then immersed into the ethanolic C12T solution and the S 2p XPS spectrum was measured again (Figure 8b). We again obtain a rather broad peak to some extent similar in shape to the one that was obtained in direct C12T adsorption on Pd, though it is somewhat narrower. Interestingly, it was noted that the spectrum shape was modified rapidly by irradiation, and the variation between the first and last scans is shown in Figure 8c,d along with fits.

The XPS spectrum in the Pd 3d region changed from the one obtained on the annealed PdS surface (Figure 2c), and the two are compared in Figure 7c. A fit of the modified Pd 3d spectrum is also shown, and we now need to include an extra sulfide Pd_{S2} component at a lower energy just as for the C12T-exposed pristine Pd surface (Figure 7a). A small Pd bulk component is included in the fit.

We fitted the spectra using several doublets of the same width. A narrower line shape was used, which reproduces also the S 2p peak after annealing in Figure 3a, and which allows reproducing the sharper low-energy rise in the C12T spectrum in this case. We assign the lower-energy 161.8 eV peak, not present in the PdS spectrum, to the thiolate. Rather than obtaining a spectrum that would be due to two doublets due to this C12T thiolate and the sharp doublet due to the $\sqrt{7}$ PdS surface at 162.53 eV, we had to employ three other doublets. Those dublets were at 162.35 and 162.96 eV, as well as a smaller one at 163.5 eV. It is possible that the 162.35 and 162.96 eV peaks are due to the PdS layer that is somewhat modified. This would correlate with the change in the Pd 3d level spectra as discussed for Figure 7c, in which an additional sulfide component is included as compared to the PdS surface case.

This fit was used for both the first scan (Figure 8c) and last scan (Figure 8d), which is modified by irradiation. It is interesting that irradiation affects the relative intensity of the 162.9 and 163.5 eV peaks (see also Supporting Information Figure S5). The latter could be due to thiol damage, whereas the change in the former suggests rearrangement in the surface sulfide if our attribution is indeed correct. A general increase in the S peaks is observed, also suggesting some thiol desorption and thinning of the layer (Figure S5).

Thus, these spectra suggest that the thiol adsorption on the PdS layer is accompanied by some modifications of the $\sqrt{7}$ PdS structure. The calculations of Carro et al.,[41] mentioned in the introduction, do suggest that thiol adsorption on this PdS layer is accompanied by some Pd atom extraction and thiol adsorption involving these Pd adatoms. This could lead to changes in S atom environment and thus affects the CLBEs. Our observations thus tend to support such changes, though no more definite conclusions can be drawn.

We would thus conclude that the low-energy shoulder is due to the thiolate and the central part is due to the sulfide interface layer. This attribution is contrary to earlier proposals,[11,34] in

dx.doi.org/10.1021/jp507051q | J. Phys. Chem. C 2014, 118, 24983−24994

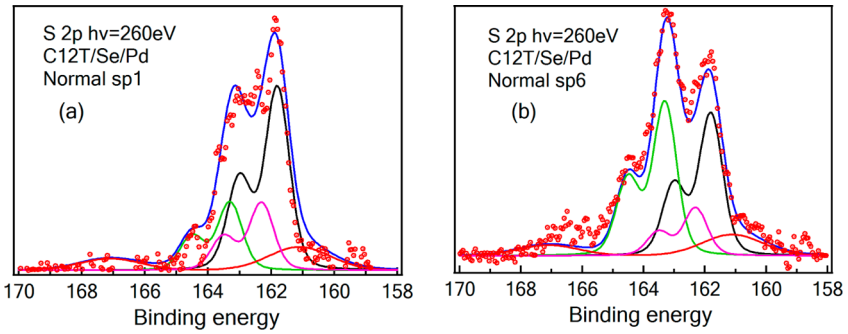

Figure 9. S 2p XPS spectrum (a) first scan (sp1) and (b) sixth scan (sp6). Lines correspond to fits described in the text.

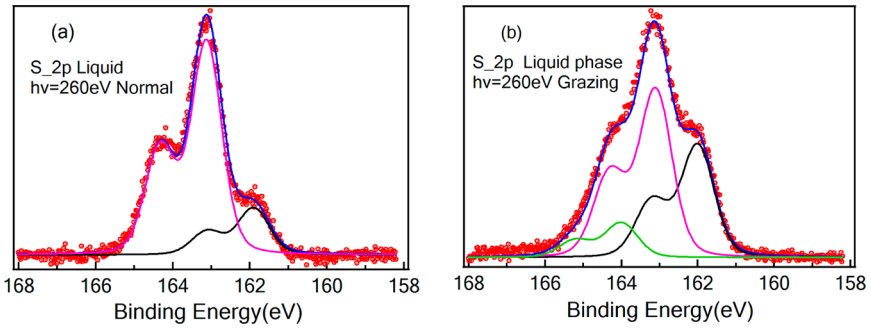

Figure 10. XPS spectra in the S 2p region for (a) normal and (b) 15° grazing emission angles taken at a 260 eV photon energy for liquid-phase adsorption of BDMT. The lines are results of fits described in the text.

which the central peak was attributed to the thiolate. As will be seen below, somewhat similar spectra are obtained with BDMT, and from their analysis one could conclude that the lower-energy part of the spectrum corresponds to a more outer sulfur atom. In this case, it supports the attribution of this structure to the thiolate. As noted in the introduction, in many cases of thiol adsorption on metals and semiconductors the thiolate binding energy is closer to 162 eV. Thus, our attribution is more consistent with this general trend.

C12T on PdSe. To get some additional insight into this interface problem, we performed a similar experiment but preadsorbed Se and formed a PdSe layer as described above by first immersing into Na_2Se and then annealing to 500 °C. While this is not equivalent to having a PdS layer, it was intriguing to see what changes would occur.

The resulting S 2p spectrum is shown in Figure 9. It has a prominent peak at 161.8 eV. Lines in Figure 9a correspond to a fit of the spectrum in which the main peak is at 161.8 eV and the two broader higher- and lower-lying components (red line) correspond to the Se 3p contribution. These are based on the fit of the Se 3p peaks in Supporting Information Figure S2.

The XPS spectrum in the Pd 3d region changed from the one obtained on the annealed PdSe surface (Figure 5c), and the two are compared in Figure 7c. A fit of the modified Pd 3d spectrum is also shown and now includes a modified sulfide $Pd_{S/Se}$ component at 335 eV instead of the earlier present smaller 335.2 eV component due to Pd_{Se}. A small Pd bulk component is included in the fit. The new 335 eV $Pd_{S/Se}$ energy position is the same as for the case of C12T on Pd and PdS. We label it as $Pd_{S/Se}$ because it could contain a small contribution from a selenide component (Figure 7a). This change may be related to changes in the Se 3d spectra described below.

We noticed that the spectrum was affected by the X-ray beam, resulting in a strong increase in the 163.3 eV component in Figure 9b. The spectrum in Figure 9a was obtained after the first scan, whereas the one in Figure 9b was obtained after six scans (see also Supporting Information Figure S5). As is known from the literature, irradiation of alkanethiol components leads to the appearance of free alkanethiols trapped within the SAM that may also be −S−S bonded, and this leads to the appearance of a radiation damage-induced structure at about this energy. One can thus conclude that the initial spectrum might have a small contribution from radiation damage also. In the fits, the green line peak at 163.3 corresponds to what becomes mainly a damage-related structure. A good fit required the introduction of a smaller doublet at about 162.3 eV. However, clearly these spectra show that the main thiolate component is at the lower 161.8 eV energy. A general increase in the Se peaks is observed, also suggesting some thiol desorption and thinning of the layer (Figure S5).

We now turn to the Se 3d spectrum. Here we observe that the quite prominent component at 53.9 eV, which we attributed above to outer Se, was strongly attenuated as though it was displaced by the thiol. As noted above, C12T adsorption here also affects the Pd 3d level binding energy. The C12T is thus adsorbed on the modified PdSe surface layer, with the thiolate component mainly at 161.8 eV. This again tends to support our assignment of the thiolate component for C12T adsorption on Pd and PdS.

Whereas the S 2p spectrum changes because of X-ray damage, no changes in these Se 3d XPS spectra were observed.

■ BDMT ADSORPTION ON PD(111)

Because self-assembly of dithiols is of interest in a number of applications, we also investigated BDMT adsorption on Pd(111) both by TOF-DRS and photoemission studies. This was done for adsorption in both liquid phase and vapor phase.

dx.doi.org/10.1021/jp507051q | J. Phys. Chem. C 2014, 118, 24983−24994

The XPS spectra of Pd 3d region are analyzed in the Supporting Information. S 2p core level spectra taken at normal angle emission and grazing angle emission taken at 260 eV photon energy from liquid phase are shown in Figure 10. As shown in Figure 10a, the spectrum is fitted using two doublets, 161.9 eV (black line) and 163.12 eV (pink line). In adsorption on Au, a standing-up phase of BDMT is characterized by a spectrum (measured at 260 eV photon energy) which looks very similar to the one in Figure 10a, with a dominant peak at about 163.1 eV. One would then be tempted to say that we do in fact form a good standing-up phase of BDMT. The 161.9 eV doublet would correspond to S bonded to the Pd surface, whereas the 163.12 eV doublet would be assigned to a free −SH group. However, the spectrum measured for grazing emission shows that the 161.9 eV peak becomes more prominent as opposed to what one would expect for emission from S atoms below the BDMT layer. In a different experiment, the spectrum looked somewhat different with a less prononced central peak (Supporting Information Figure S7a,b). In fact, in this case the spectrum looked very similar to the one for sulfur adsorption in Figure 3. Given these similarities and the strong sulfidation character of the Pd 3d peak, we would tend to conclude that what we see is a thiolate layer on a Pd sulfide. Experiments in heated *n*-hexane following the protocol for Au[35,58] did not yield better results.

We also performed experiments for vapor-phase adsorption. The XPS spectra of S 2p core level structure measured at normal emission angle and grazing emission angle are shown in Supporting Information Figure S7c,d. Here we found that the 162 eV peak was more intense. In grazing emission the central peak appears somewhat more prominent, pointing possibly to some free −SH from standing BDMT.

To gain further insight, we performed TOF-DRS measurements on the Orsay setup. The Pd(111) surface after cleaning was exposed to a large dose of BDMT. The resulting TOF-DRS spectrum is shown in Figure 11 and compared with that for a clean Pd surface and one obtained for a Au surface under similar exposure conditions. As labeled in the figure, in these spectra we observe features due to recoiled (fast forward ejected) H and C atoms and at longer flight times a broad structure due to Ar multiply scattered on the organic layer. For the Au surface one sees an extra prominent sharp structure which is assigned to recoiled S atoms from the top of the standing-up BDMT layer[62] and a feature due to Ar scattered from the top SAM S atoms. As may be seen, as opposed to the Au case, for Pd we do not see a very prominent peak attributable to S, but only a very small structure. This observation agrees with our conclusion that we do not form a predominantly S-terminated standing-up BDMT layer. The TOF spectra on BDMT do indicate that the layer is thick because no sharp structure due to scattering off the Pd substrate is observable at the position indicated by the arrow. We observed that heating the sample above 200 °C leads to partial desorption of BDMT, but at higher temperatures a large amount of carbon remained on the surface (see Supporting Information Figure S8).

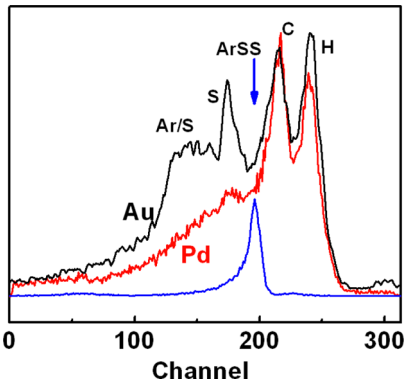

Figure 11. TOF-DRS spectra for 4 keV Ar incident at 7° on the BDMT on Au and BDMT on Pd surfaces. The arrow indicates the position of Ar single scattering on the clean Pd substrate. The corresponding spectrum profile is also shown (blue line).

SUMMARY

In this work we investigated the important problem of the interface in self-assembly of an alkanethiol and BDMT adsorption on Pd. Because earlier works pointed to the fact that alkanethiols assemble not on Pd but on a PdS interface layer formed in the initial phases of adsorption, as a complement we also studied sulfur and also selenium chemisorption to have a clearer idea of the characteristics of palladium sulfide and selenide surface layers. The main aspects of our findings are delineated below.

(1) Initial S atom adsorption on the Pd(111) surface leads to appearance of two Pd sulfide components with different Pd 3d CLBEs. The S 2p peak consists of an outer lying 161.7 eV (S $2p_{3/2}$) component and an underlying component at 162.68 eV. Annealing causes loss of sulfur and formation of a surface PdS layer, for which a single sufide Pd 3d component lying at about 0.6 eV higher than the bulk Pd 3d CLBE is observed. The S 2p peak then shows just one sharp doublet at 162.47 eV. From the LEED pattern, we conclude that a PdS $\sqrt{7}$ structure is observed; thus, the S 2p CLBE corresponds to this structure.

(2) For initial selenization, there appear two selenide components with different Pd 3d CLBEs. The Se 3d peak has dominantly a two doublet component structure, corresponding to a surface selenide layer with a "lower" component and another more "surface" component. After the sample was annealed, the LEED showed a pattern overall similar to the sulfur case, but a more complex one with widely spaced domains, and the XPS spectra showed persistence of a multicomponent structure with an underlying component and another more "surface" component.

(3) In the case of C12T adsorption on Pd(111), we observe a multicomponent S 2p peak with a lower-energy doublet at 161.7 eV due to thiolate S, corresponding to molecules adsorbed on a PdS layer in which the S 2p binding energy corresponds to the higher-energy doublet at 162.78 eV. This is different from earlier assignments of structures in these energy ranges.[11,34] For C12T adsorption on a $\sqrt{7}$ PdS layer, results are similar to the Pd(111) case, but the spectral features are narrower. The thiolate component could be defined without ambiguity as lying at 161.8 eV. The sulfide layer appeared to be composed of two components with slightly different S 2p CLBEs and distinct from the CLBE of the original PdS layer. Adsorption of C12T on PdS led to changes in the Pd 3d CLBEs.

(4) These experiments suggest that the thiol adsorption on the PdS layer is accompanied by modifications of the $\sqrt{7}$ PdS structure and would support calculations of Carro et al.[41] that indicate thiol adsorption on this PdS layer is accompanied by

dx.doi.org/10.1021/jp507051q | J. Phys. Chem. C 2014, 118, 24983−24994

some Pd atom extraction and thiol adsorption involves these Pd adatoms.

(5) C12T adsorption on a selenized surface reveals thiol adsorption with thiolate binding energy of 161.8 eV, similar to the sulfidized surface. Changes in the Se 3d peak due to replacement of an outer surface component by the thiol are observed. Our assignment of the lower binding energy structure to the thiolate both in this case and in the case of adsorption on Pd and PdS is consistent with known thiol adsorption on metals and also on GaAs and InP in which the thiolate binding energy is close to 162 eV. This differs from earlier assignments.[11,34]

(6) In the case of C12T adsorption on PdS and PdSe, rapid damage by X-ray irradiation occurs and led to the appearance of a higher-energy component at 163.5 eV and interestingly also increased the intensity of one of the components assigned to the sulfide layer. Some desorption of the thiol also appears to occur, resulting in thinning of the layer.

(7) For BDMT adsorption, the S 2p spectra and modifications in Pd 3d core level are similar to those of the C12T case. We do not see much evidence of free −SH that would signify a standing-up SAM of BDMT. The reason for this is not very clear. There is a possibility that when BDMT reacts with the surface, one −SH end reacts to give the PdS layer and the other end then adsorbs on the reacted surface leaving a molecule without an −SH end group. This would then hinder formation of a thiol-terminated standing-up BDMT SAM.

We hope that this study will contribute to further understanding of the complex interface in chalcogenide SAM formation on reactive substrates. Calculations on the CLBEs for thiols on Pd as in the work of Carro et al.,[41] which however does not cite these, would help in the understanding of some of the interesting features in our results. Theoretical studies of Se adsorption would help in understanding the apparently more complex nature of the PdSe layer.

■ ASSOCIATED CONTENT

Supporting Information

XPS spectra for S and Se on Pd, X-ray damage effects, valence band for PdSe, BDMT Pd 3d spectra, and adsorption and desorption by TOF-DRS. This material is available free of charge via the Internet at http://pubs.acs.org.

■ AUTHOR INFORMATION

Corresponding Author

*E-mail: vladimir.esaulov@u-psud.fr. Tel: +33-169157680.

Notes

The authors declare no competing financial interest.

■ ACKNOWLEDGMENTS

J.J. thanks the Chinese Scholarship Council for her PhD scholarship. We thank Jonathan Correa for assistance with BDMT experiments.

■ REFERENCES

(1) Astruc, D. Palladium Nanoparticles as Efficient Green Homogeneous and Heterogeneous Carbon−Carbon Coupling Pre-catalysts: A Unifying View. *Inorg. Chem.* **2007**, *46*, 1884−1894.

(2) Muæiz, K. High-Oxidation-State Palladium Catalysis: New Reactivity for Organic Synthesis. *Angew. Chem., Int. Ed.* **2009**, *48*, 2−14.

(3) Beletskaya, I. P.; Cheprakov, A. V. The Heck Reaction as a Sharpening Stone of Palladium Catalysis. *Chem. Rev. (Washington, DC, U.S.)* **2000**, *100*, 3009−3066.

(4) Barnard, C. Palladium-Catalysed C−C Coupling: Then and Now. *Platinum Met. Rev.* **2008**, *52*, 38−45.

(5) Lewis, F. A. *The Palladium Hydrogen System*; Academic Press: New York, 1967.

(6) Barton, J. C.; F. A. Lewis, F. A.; Woodward, I. Hysteresis of the Relationships between Electrical Resistance and the Hydrogen Content of Palladium. *Trans. Faraday Soc.* **1963**, *59*, 1201.

(7) Hamilton, H. PGM Highlights: Palladium-Based Membranes for Hydrogen Separation. *Platinum Met. Rev.* **2012**, *56*, 117−123.

(8) Morreale, B. D.; Ciocco, M. V.; Howard, B. H.; Killmeyer, R. P.; Cugini, A. V.; Enick, R. M. Effect of Hydrogen-Sulfide on the Hydrogen Permeance of Palladium−Copper Alloys at Elevated Temperatures. *J. Membr. Sci.* **2004**, *241*, 219−224.

(9) Miller, J. B.; Alfonso, D. R.; Howard, B. H.; O'Brien, C. P.; Bryan, D.; Morreale, B. D. Hydrogen Dissociation on Pd_4S Surfaces. *J. Phys. Chem. C* **2009**, *113*, 18800−18806.

(10) Oudar, J. Sulfur Adsorption and Poisoning of Metallic Catalysts. *Catal. Rev.: Sci. Eng.* **1980**, *22*, 171−195.

(11) Love, J. C.; Wolfe, D. B.; Chabinyc, M. L.; Paul, K. E.; Whitesides, G. M. Formation and Structure of Self-Assembled Monolayers of Alkanethiolates on Palladium. *J. Am. Chem. Soc.* **2002**, *124*, 1576−1577.

(12) Love, J. C.; Wolfe, D. B.; Haasch, R.; Chabinyc, M. L.; Paul, K. E.; Whitesides, G. M.; Nuzzo, R. G. Self-Assembled Monolayers of Alkanethiolates on Palladium are Good Etch Resists. *J. Am. Chem. Soc.* **2003**, *125*, 2597−2609.

(13) Nuzzo, R. G.; Allara, D. L. Adsorption of Bifunctional Organic Disulfides on Gold Surfaces. *J. Am. Chem. Soc.* **1983**, *105*, 4481−4483.

(14) Ulman, A. Formation and Structure of Self Assembled Monolayers. *Chem. Rev. (Washington, DC, U.S.)* **1996**, *96*, 1533−1554.

(15) Schreiber, F. Structure and Growth of Self Assembling Monolayers. *Prog. Surf. Sci.* **2000**, *65*, 151−256.

(16) Woodruff, D. P. The Interface Structure of n-Alkylthiolate Self-Assembled Monolayers on Coinage Metal Surfaces. *Phys. Chem. Chem. Phys.* **2008**, *10*, 7211−7221.

(17) Guo, G.; Zheng, W.; Hamoudi, H.; Dablemont, C.; Esaulov, V. A.; Bourguignon, B. On the Chain Length Dependence of CH_3 Vibrational Mode Relative Intensities in Sum Frequency Generation Spectra of Self Assembled Alkanethiols. *Surf. Sci.* **2008**, *602*, 3551−3559.

(18) Prato, M.; Moroni, R.; Bisio, F.; Rolandi, R.; Mattera, L.; Cavalleri, O.; Canepa, M. Optical Characterization of Thiolate Self-Assembled Monolayers on Au(111). *J. Phys. Chem. C* **2008**, *112*, 3899−3906.

(19) Cookson, J. The Preparation of Palladium Nanoparticles. *Platinum Met. Rev.* **2012**, *56*, 83−98.

(20) Marshall, S. T.; O'Brien, M.; Oetter, B.; Corpuz, A.; Richards, R. M.; Schwartz, D. K.; Medlin, J. W. Controlled Selectivity for Palladium Catalysts Using Self-Assembled Monolayers. *Nat. Mater.* **2010**, *9*, 853−858.

(21) Yamauchi, M.; Ikeda, R.; Kitagawa, H.; Takata, M. Nanosize Effects on Hydrogen Storage in Palladium. *J. Phys. Chem. C* **2008**, *112*, 3294−3299.

(22) Horinouchi, S.; Yamanoi, Y.; Yonezawa, T.; Mouri, T.; Nishihara, H. Hydrogen Storage Properties of Isocyanide-Stabilized Palladium Nanoparticles. *Langmuir* **2006**, *22*, 1880−1884.

(23) Mubeen, S.; Zhang, T.; Yoo, B.; Deshusses, M. A.; Myung, N. V. Palladium Nanoparticles Decorated Single-Walled Carbon Nanotube Hydrogen Sensor. *J. Phys. Chem. C* **2007**, *111*, 6321−6327.

(24) Tobiška, P.; Hugon, O.; Trouillet, A.; Gagnaire, H. An Integrated Optic Hydrogen Sensor Based on SPR on Palladium. *Sens. Actuators, B* **2001**, *74*, 168−172.

(25) Zelakiewicz, B. S.; Lica, G. C.; Deacon, M. L.; Tong, Y. Y. ^{13}C NMR and Infrared Evidence of a Dioctyl−Disulfide Structure on Octanethiol-Protected Palladium Nanoparticle Surfaces. *J. Am. Chem. Soc.* **2004**, *126*, 10053−10058.

(26) Ramallo-López, J. M.; Giovanetti, L.; Craievich, A. F.; Vicentin, F. C.; Marín-Almazo, M.; José-Yacaman, M.; Requejo, F. G. XAFS, SAXS and HREM Characterization of Pd Nanoparticles Capped with *n*-Alkyl Thiol Molecules. *Phys. B (Amsterdam, Neth.)* **2007**, *389*, 150−154.
(27) Corthey, G.; Rubert, A. A.; Picone, A. L.; Casillas, G.; Giovanetti, LJ.; Ramallo-López, J. M.; Zelaya, E.; Benitez, G. A.; Requejo, F. G.; José-Yacamán, M.; et al. New Insights into the Chemistry of Thiolate-Protected Palladium Nanoparticles. *J. Phys. Chem. C* **2012**, *116*, 9830−9837.
(28) Liu, Y.; Sun, C.; Bolin, T.; Wu, T.; Liu, Y.; Sternberg, M.; Sun, S.; Lin, X. M. Kinetic Pathway of Palladium Nanoparticle Sulfidation Process at High Temperatures. *Nano Lett.* **2013**, *13*, 4893−4901.
(29) Brust, M.; Blass, P. M.; Bard, A. J. Self-Assembly of Photoluminescent Copper(I)−Dithiol Multilayer Thin Films and Bulk Materials. *Langmuir* **1997**, *13*, 5602−5607.
(30) Hamoudi, H.; Ariga, K.; Uosaki, K.; Esaulov, V. A. Going Beyond The Self-Assembled Monolayer: Metal Intercalated Dithiol Multilayers and Their Conductance. *RSC Adv.* **2014**, *4*, 39657−39666.
(31) Hamoudi, H. Bottom-up Nanoarchitectonics of Two-Dimensional Freestanding Metal Doped Carbon Nanosheet. *RSC Adv.* **2014**, *4*, 22035−22041.
(32) Jia, J.; Mukherjee, S.; Hamoudi, H.; Nannarone, S.; Pasquali, L.; Esaulov, V. A. Lying-Down to Standing-Up Transitions in Self Assembly of Butanedithiol Monolayers on Gold and Substitutional Assembly by Octanethiols. *J. Phys. Chem. C* **2013**, *117*, 4625−4631.
(33) Chaudhari, V.; Harish, M. N. K.; Srinivasan, S.; Esaulov, V. A. Substitutional Self-Assembly of Alkanethiol and Selenol SAMs from a Lying-Down Doubly Tethered Butanedithiol SAM on Gold. *J. Phys. Chem. C* **2011**, *115*, 16518−16523.
(34) Corthey, G.; Rubert, A. A.; Benitez, G. A.; Fonticelli, M. H.; Salvarezza, R. C. Electrochemical and X-ray Photoelectron Spectroscopy Characterization of Alkanethiols Adsorbed on Palladium Surfaces. *J. Phys. Chem. C* **2009**, *113*, 6735−6742.
(35) Hamoudi, H.; Prato, M.; Dablemont, C.; Cavalleri, O.; Canepa, M.; Esaulov, V. A. Self-Assembly of 1, 4-Benzenedimethanethiol Self-Assembled Monolayers on Gold. *Langmuir* **2010**, *26*, 7242−7247.
(36) Millone, M. A. D.; Hamoudi, H.; Rodriguez, L.; Rubert, A.; Benitez, G. A.; Vela, M. E.; Salvarezza, R. C.; Gayone, J. E.; Sanchez, E. A.; Grizzi, O.; et al. Self-assembly of Alkanedithiols on Au(111) From Solution: Effect of Chain Length and Self-assembly Conditions. *Langmuir* **2009**, *25*, 12945−12953.
(37) Hamoudi, H.; Guo, Z. A.; Prato, M.; Dablemont, C.; Zheng, W. Q.; Bourguignon, B.; Canepa, M.; Esaulov, V. A. On the Self Assembly of Short Chain Alkanedithiols. *Phys. Chem. Chem. Phys.* **2008**, *10*, 6836−6841.
(38) Love, J. C.; Estro, L. A.; Kriebel, J. K.; Nuzzo, R. G.; Whitesides, G. M. *Chem. Rev. (Washington, DC, U.S.)* **2005**, *105*, 1103−1170.
(39) McGuiness, C. L.; Shaporenko, A.; Zharnikov, M.; Walker, A. V.; Allara, D. L. Molecular Self-Assembly at Bare Semiconductor Surfaces: Investigation of the Chemical and Electronic Properties of the Alkanethiolate−GaAs(001) Interface. *J. Phys. Chem. C* **2007**, *111*, 4226−4234.
(40) Rodriguez, J. A.; Dvorak, J.; Jirsak, T.; Liu, G.; Hrbek, J.; Aray, Y.; Gonzalez, C. Coverage Effects and the Nature of the Metal-Sulfur Bond in S/Au(111): High-Resolution Photoemission and Density-Functional Studies. *J. Am. Chem. Soc.* **2003**, *125*, 276−285.
(41) Carro, P.; Corthey, G.; Rubert, A. A.; Benitez, G. A.; Fonticelli, M. H.; Salvarezza, R. C. The Complex Thiol−Palladium Interface: A Theoretical and Experimental Study. *Langmuir* **2010**, *26*, 14655−14662.
(42) Rodriguez, J. A.; Chaturvedi, S.; Jirsak, T. The Bonding of Sulfur to Pd Surfaces: Photoemission and Molecular−Orbital Studies. *Chem. Phys. Lett.* **1998**, *296*, 421−428.
(43) Maca, F.; Scheffler, M.; Berndt, W. The Adsorption of Sulphur on Pd(111) I. A LEED Analysis of the (2 × 3)R30° S Adsorbate Structure. *Surf. Sci.* **1985**, *160*, 467−474.
(44) Grillo, M.; Stampfl, C.; Berndt, W. Low-Energy Electron-Diffraction Analysis of the $(\sqrt{7} \times \sqrt{7})$R19.1°-S Adsorbate Structure on the Pd(111) surface. *Surf. Sci.* **1994**, *317*, 84−98.
(45) Patterson, C.; Lambert, R. Structure and Properties of the Palladium/Sulfur Interface: S_2 Chemisorption on Pd(111). *Surf. Sci.* **1987**, *187*, 339−358.
(46) Forbes, J. G.; Gellman, A. J.; Dunphy, J. C.; Salmeron, M. Imaging of Sulfur Overlayer Structures on the Pd(111) surface. *Surf. Sci.* **1992**, *279*, 68−78.
(47) Liu, W.; Mitchell, K.; Berndt, W. The structure of the Pd(111)-$(\sqrt{7} \times \sqrt{7})$R19.1° -S Surface: Comparison with the Corresponding P/Rh(111) Surface. *Surf. Sci.* **1997**, *393*, L119−L125.
(48) Dhanak, V.; Shard, A.; Cowie, B.; Santoni, A. The Structures of Sulphur on Pd(111) Studied by X-ray Standing Wavefield Absorption and Surface EXAFS. *Surf. Sci.* **1998**, *410*, 321−329.
(49) Speller, S.; Rauch, T.; Bömermann, J.; Borrmann, P.; Heiland, W. Surface Structures of S on Pd(111). *Surf. Sci.* **1999**, *441*, 107−116.
(50) Speller, S.; Rauch, T.; Postnikov, A.; Heiland, W. Scanning Tunneling Microscopy and Spectroscopy of S on Pd. *Phys. Rev. B: Condens. Matter Mater. Phys.* **2000**, *61*, 7297−7300.
(51) Alfonso, D. A.; Cugini, A. V.; Sholl, D. S. Density Functional Theory Studies of Sulfur Binding on Pd, Cu and Ag and Their Alloys. *Surf. Sci.* **2003**, *546*, 12−26.
(52) Alfonso, D. R. First-Principles Study of Sulfur Overlayers on Pd(111) Surface. *Surf. Sci.* **2005**, *596*, 229−241.
(53) Mullins, D. R.; Lyman, P. F. Adsorption and Reaction of Methanethiol on Tungsten(001). *J. Phys. Chem.* **1993**, *97*, 9226−9232.
(54) Mullins, D. R.; Lyman, P. F. Adsorption and Reaction of Methanethiol on Ruthenium(0001). *J. Phys. Chem.* **1993**, *97*, 12008−12013.
(55) Rufael, T. S.; Huntley, D. R.; Mullins, D. R.; Gland, J. L. Methyl Thiolate on Ni(111): Multiple Adsorption Sites and Mechanistic Implications. *J. Phys. Chem.* **1995**, *99*, 11472−11480.
(56) Vollmer, S.; Witte, G.; Wöll, Ch. Structural Analysis of Saturated Alkanethiolate Monolayers on Cu(100): Coexistence of Thiolate and Sulfide Species. *Langmuir* **2001**, *17*, 7560−7565.
(57) Alarcon, L. S.; Jia, J.; Carrera, A.; Esaulov, V.; Ascolani, H.; Gayone, J.; Sanchez, E.; Grizzi, O. Direct recoil Spectroscopy of Adsorbed Atoms and Self-Assembled Monolayers on Cu(001). *Vacuum* **2014**, *105*, 80−87.
(58) Pasquali, L.; Terzi, F.; Seeber, R.; Nannarone, S.; Datta, D.; Dablemont, C.; Hamoudi, H.; Canepa, M.; Esaulov, V. A. UPS, XPS, and NEXAFS Study of Self-Assembly of Standing 1,4-Benzenedimethanethiol SAMs on Gold. *Langmuir* **2011**, *27*, 4713−4720.
(59) Pasquali, L.; Mukherjee, S.; Terzi, F.; Giglia, A.; Mahne, N.; Koshmak, K.; Esaulov, V. A.; Toccafondi, C.; Canepa, M.; Nannarone, S. Structural and Electronic Properties of Anisotropic Ultrathin Organic Films from Dichroic Resonant Soft X-ray Reflectivity. *Phys. Rev. B: Condens. Matter Mater. Phys.* **2014**, *89*, 045401.
(60) Jia, J.; Bendounan, A.; Harish, M. N. K.; Chaouchi, K.; Sirotti, F.; Sampath, S.; Esaulov, V. A. Selenium Adsorption on Au(111) and Ag(111) Surfaces: Adsorbed Selenium and Selenide Films. *J. Phys. Chem. C* **2013**, *117*, 9835−9842.
(61) Esaulov V. A. Low Energy Ion Scattering and Recoiling Spectroscopy in Surface Science. In *Surface Science Techniques*; Bracco G., Holst, B., Eds.; Springer Series in Surface Science; Springer: Berlin, 2013; Vol. *51*, pp 423−460.
(62) Alarcón, L. S.; Chen, L.; Esaulov, V. A.; Gayone, J. E.; Sánchez, E. A.; Grizzi, O. Thiol Terminated 1,4-Benzenedimethanethiol Self-Assembled Monolayers on Au(111) and InP(110) from Vapor Phase. *J. Phys. Chem. C* **2010**, *114*, 19993−19999.
(63) Andersen, J. N.; Hennig, D.; Lundgren, E.; Methfessel, M.; R. Nyholm, R.; Scheffler, M. Surface Core-Level Shifts of Some 4d-Metal Single-Crystal Surfaces: Experiments and ab Initio Calculations. *Phys. Rev. B: Condens. Matter Mater. Phys.* **1994**, *50*, 17525−17533.
(64) Gronbeck, H.; Klacar, S.; Martin, N. M.; A. Hellman, A.; Lundgren, E.; Andersen, J. N. Mechanism for Reversed Photoemission Core-Level Shifts of Oxidized Ag. *Phys. Rev. B: Condens. Matter Mater. Phys.* **2012**, *85*, 115445.

(65) Ma, Y.; Rudolf, P.; Chaban, E. E.; Chen, C. T.; Meigs, G.; Sette, P. Multiple Sulfur Sites in the Cu(100)p(2×2)-S Surface Structure. *Phys. Rev. B: Condens. Matter Mater. Phys.* **1990**, *41*, 5424.
(66) Jia, J.; Bendounan, A.; Chaouchi, K.; Esaulov, V. A. Sulfur Interaction with Cu(100) and Cu(111) Surfaces: A Photoemission Study. *J. Phys. Chem. C* **2014**, DOI: 10.1021/jp5078517.